CCI+ PHASE 2 – NEW ECVS

PERMAFROST

D2.2 ALGORITHM THEORETICAL BASIS DOCUMENT (ATBD)

VERSION 5.0

15 NOVEMBER 2024

PREPARED BY

Document Status Sheet

Issue	Date	Details	Authors
1.0	28.02.2019	First version	SW, AB, TS
2.0	30.11.2019	Update of description of input data (stratigraphy)	SW, AB
3.0	30.11.2020	Update on year 3 processing chain, demonstrator product for use of temperature_cci and snow_cci data; extension of spin-up period	SW, AB
4.0	31.05.2023	Extension of model spin-up description, description of changes of model components, input data (LST_cci) and output grid	SW, AB
5.0	15.11.2024	Updates on model components and input data (LST_cci, landcover)	SW, AB

Author team

Sebastian Westermann, GUIO

Annett Bartsch, B.GEOS

Tazio Strozzi, GAMMA

ESA Technical Officer:

Frank Martin Seifert

TABLE OF CONTENTS

EXECUTIVE SUMMARY

This document provides a detailed description of the algorithm chosen to generate the Permafrost ECV products to be delivered in the Permafrost_cci project. The processing chain is described, including pre-processing of input data, the main processing steps using the ground thermal model CryoGrid CCI, and post-processing of model results. In CCI4 iteration 1, CryoGrid CCI has been fully integrated in the CryoGrid community model (Westermann et al., 2023), making it accessible to a wider user community of permafrost researchers. CryoGrid CCI is a ground thermal model based on existing permafrost models, which is optimized for efficient computation to facilitate application for the entire permafrost domain. For each pixel, a model ensemble is computed in order to simulate the considerable subgrid variability (1km resolution) of the ground thermal regime observed in field-based studies. The model ensemble takes the spatial variability of landcover and ground stratigraphy, as well as snow depth into account, what allows for computation of a permafrost fraction. At the boundary of the permafrost domain, this makes it possible to quantitatively reproduce the well-established zonations in discontinuous and sporadic permafrost. The processing chain makes use of remotely sensed land surface temperatures (LST data from MODIS) and landcover (ESA CCI), which is supplemented within Permafrost_cci by a range of ancillary information, such as ground stratigraphies and fields of the ERA-5 reanalysis. The spin-up of the ground thermal profile is achieved by using reanalysis data from 1951 to 1980 which are statistically downscaled with MODIS LST using an overlap period from 2003 to 2021. Furthermore, the model is run twice for the five year period 1980 to 1984, allowing for the ground temperatures in the active layer and the uppermost permafrost to stabilize. The CryoGrid CCI model delivers the thermal profile from the surface downwards at sufficient temporal resolution to resolve the seasonal cycle. The output variables computed from the model state are mean annual ground temperature at different depths, annual active layer thickness and permafrost fraction within 1km pixels. Furthermore, instantaneous ground temperatures is provided at four different times in a year allowing to capture the seasonal temperature signal. The output is provided in geographic coordinates with a base resolution of 0.01 degrees, making it compatible to other products in the CCI family.

1 INTRODUCTION

1.1 Purpose of the document

The parameters required by the Global Climate Observing System (GCOS) for the Essential Climate Variable (ECV) Permafrost are Depth of Active Layer (the seasonal thaw layer) and Permafrost Temperature. ESA Permafrost_cci will provide the 'core' ECV product Permafrost Temperature and the two 'side' ECV products Permafrost Active Layer and Permafrost Extent.

This document details the theoretical basis of the Permafrost_cci algorithm designed to deliver the Permafrost ECV products.

1.2 Structure of the document

This document contains a glossary of permafrost specific terms in section 1.7. Section 2 describes the the scientific background of the Permafrost_cci algorithm. The remaining sections detail the theoretical and practical background of the selected algorithm, including input and output data as well as treatment of uncertainties.

1.3 Applicable Documents

[AD-1] ESA 2017: Climate Change Initiative Extension (CCI4) Phase 1 – New Essential Climate Variables - Statement of Work. ESA-CCI-PRGM-EOPS-SW-17-0032

[AD-2] Requirements for monitoring of permafrost in polar regions - A community white paper

in response to the WMO Polar Space Task Group (PSTG), Version 4, 2014-10-09. Austrian Polar Research Institute, Vienna, Austria, 20 pp

[AD-3] ECV 9 Permafrost: assessment report on available methodological standards and guides,

1 Nov 2009, GTOS-62

[AD-4] GCOS-200, the Global Observing System for Climate: Implementation Needs (2016

GCOS Implementation Plan, 2015.

1.4 Reference Documents

[RD-1] Bartsch, A., Matthes, H., Westermann, S., Heim, B., Pellet, C., Onacu, A., Strozzi, T.(2024): ESA CCI+ Permafrost User Requirements Document, v4.0

[RD-2] Bartsch, A., Westermann, Strozzi, T., Wiesmann, A., Kroisleitner, C. (2024): ESA CCI+ Permafrost Product Specifications Document, v5.0

[RD-3] Bartsch, A., Westermann, S., Heim, B., Wieczorek, M., Pellet, C., Barboux, C., Kroisleitner, C., Strozzi, T. (2020): ESA CCI+ Permafrost Data Access Requirements Document, v2.0

[RD-4] Bartsch, A.; Grosse, G.; Kääb, A.; Westermann, S.; Strozzi, T.; Wiesmann, A.; Duguay, C.; Seifert, F. M.; Obu, J.; Goler, R.: GlobPermafrost – How space-based earth observation supports understanding of permafrost. Proceedings of the ESA Living Planet Symposium, pp. 6.

[RD-5] IPA Action Group 'Specification of a Permafrost Reference Product in Succession of the IPA Map' (2016): Final report.

https://ipa.arcticportal.org/images/stories/AG_reports/IPA_AG_SucessorMap_Final_2016.pdf

[RD-6] Westermann, S., Bartsch, A., Strozzi, T. (2025): ESA CCI+ Product Validation and Assessment Report, v5.0

1.5 Bibliography

A complete bibliographic list that support arguments or statements made within the current document is provided in Section 9.1.

1.6 Acronyms

A list of acronyms is provided in section 9.2.

1.7 Glossary

The list below provides a selection of term relevant for the parameters addressed in CCI4 Permafrost. A comprehensive glossary is available as part of the Product Specifications Document [RD-2].

active-layer thickness

The thickness of the layer of the ground that is subject to annual thawing and freezing in areas underlain by permafrost.

The thickness of the active layer depends on such factors as the ambient air temperature, vegetation, drainage, soil or rock type and total water content, snowcover, and degree and orientation of slope. As a rule, the active layer is thin in the High Arctic (it can be less than 15 cm) and becomes thicker farther south (1 m or more).

The thickness of the active layer can vary from year to year, primarily due to variations in the mean annual air temperature, distribution of soil moisture, and snowcover.

The thickness of the active layer includes the uppermost part of the permafrost wherever either the salinity or clay content of the permafrost allows it to thaw and refreeze annually, even though the material remains cryotic (T < 0°C).

Use of the term "depth to permafrost" as a synonym for the thickness of the active layer is misleading, especially in areas where the active layer is separated from the permafrost by a residual thaw layer, that is, by a thawed or noncryotic (T > 0°C) layer of ground.

REFERENCES: Muller, 1943; Williams, 1965; van Everdingen, 1985

continuous permafrost

Permafrost occurring everywhere beneath the exposed land surface throughout a geographic region with the exception of widely scattered sites, such as newly deposited unconsolidated sediments, where the climate has just begun to impose its influence on the thermal regime of the ground, causing the development of continuous permafrost.

For practical purposes, the existence of small taliks within continuous permafrost has to be recognized. The term, therefore, generally refers to areas where more than 90 percent of the ground surface is underlain by permafrost.

REFERENCE: Brown, 1970.

discontinuous permafrost

Permafrost occurring in some areas beneath the exposed land surface throughout a geographic region where other areas are free of permafrost.

Discontinuous permafrost occurs between the continuous permafrost zone and the southern latitudinal limit of permafrost in lowlands. Depending on the scale of mapping, several subzones can often be distinguished, based on the percentage (or fraction) of the land surface underlain by permafrost, as shown in the following table.

Permafrost	English usage	Russian Usage
Extensive	65-90%	Massive Island

Intermediate	35-65%	Island
Sporadic	10-35%	Sporadic
Isolated Patches	0-10%	-

SYNONYMS: (not recommended) insular permafrost; island permafrost; scattered permafrost.

REFERENCES: Brown, 1970; Kudryavtsev, 1978; Heginbottom, 1984; Heginbottom and Radburn, 1992; Brown et al., 1997.

mean annual ground temperature (MAGT)

Mean annual temperature of the ground at a particular depth.

The mean annual temperature of the ground usually increases with depth below the surface. In some northern areas, however, it is not un-common to find that the mean annual ground temperature decreases in the upper 50 to 100 metres below the ground surface as a result of past changes in surface and climate conditions. Below that depth, it will increase as a result of the geothermal heat flux from the interior of the earth. The mean annual ground temperature at the depth of zero annual amplitude is often used to assess the thermal regime of the ground at various locations.

permafrost

Ground (soil or rock and included ice and organic material) that remains at or below 0°C for at least two consecutive years .

Permafrost is synonymous with perennially cryotic ground: it is defined on the basis of temperature. It is not necessarily frozen, because the freezing point of the included water may be depressed several degrees below 0°C; moisture in the form of water or ice may or may not be present. In other words, whereas all perennially frozen ground is permafrost, not all permafrost is perennially frozen. Permafrost should not be regarded as permanent, because natural or man-made changes in the climate or terrain may cause the temperature of the ground to rise above 0°C.

Permafrost includes perennial ground ice, but not glacier ice or icings, or bodies of surface water with temperatures perennially below 0°C; it does include man-made perennially frozen ground around or below chilled pipelines, hockey arenas, etc.

Russian usage requires the continuous existence of temperatures below 0°C for at least three years, and also the presence of at least some ice.

SYNONYMS: perennially frozen ground, perennially cryotic ground and (not recommended) biennially frozen ground, climafrost, cryic layer, permanently frozen ground.

REFERENCES: Muller, 1943; van Everdingen, 1976; Kudryavtsev, 1978.

2   SCIENTIFIC BACKGROUND

Permafrost and frozen ground are key elements of the terrestrial cryosphere that will be strongly affected by a warming climate. With widespread permafrost degradation likely to occur in this century, remote sensing of permafrost is seeking to unveil the processes and causal connections governing this development, from the monitoring of variables related to the permafrost state to the mapping of the impacts of degradation and potential natural hazards on the ground.

Remote sensing of permafrost is challenging. The physical subsurface variables which characterize its thermal state – ground temperature, ice content and thaw depth – are not directly measurable through current remote sensing technologies. In order to gain spatially continuous information, numerical models are key. Permafrost_cci will therefore produce Level 4 datasets, based on CDRs from other ECVs [RD-2].

2.1   Monitoring of Permafrost ECV parameters

At present, terrestrial systems are in place within which these physical variables are monitored at specific sites, either continuously (as typical in boreholes for ground temperature in the GTN-P) or sporadically during a season (as for active layer thickness at CALM sites), or even only every few years. While the terrestrial monitoring has been drastically expanded during and after the "International Polar Year" (IPY), the distribution of sites is strongly biased towards a few regions (typically where resource extraction and/or infrastructure projects have created easy access), leaving vast areas uncovered by monitoring. This in particular renders upscaling of trends in the permafrost ECV to global scale problematic. Furthermore, it complicates validation of Earth System Model output for to permafrost, which causes considerable uncertainty in future projections on the permafrost-carbon feedback.

The main requirement for EO-based algorithms for permafrost ECV generation is therefore to improve the spatial and temporal coverage compared to the existing in-situ networks, while at the same time providing consistent coverage of at least all relevant permafrost regions. Since EO-based algorithms necessarily operate at the spatial scale of individual pixels, the spatial resolution of the output must be put in context with the spatial variability of permafrost temperatures and active layer thickness.

2.2   Thermal subsurface modeling

In the ESA GlobPermafrost project, a simple equilibrium permafrost model has been employed to infer ground temperatures and permafrost extent (Obu et al., 2019; 2020) based on thawing and freezing

degree days derived from remotely sensed data, in particular Land Surface Temperature (LST). This model mainly has the advantage of simplicity which makes global application possible without a high-performance computing (HPC) system. However, the transient response of the ground thermal regime to a changing climate forcing cannot be reproduced with an equilibrium scheme, and instead, transient permafrost models must be used. Such transient thermal subsurface models are widely employed in permafrost science. While they use a wide variety of forcing data sets, all state-of-the-art models rely on the same model physics, numerically solving the heat conduction equation including the phase change of water/ice in soil pores. The feasibility and maturity of transient permafrost models in conjunction with EO-data over large spatial domains has been demonstrated in a pilot study in Northern Siberia (Westermann et al., 2017). EO data sets are employed to determine the upper boundary condition of the differential equation, while its coefficients (e.g. heat capacity and thermal conductivity) are selected according to landcover information (Westermann et al., 2017). With this, a spatial resolution of the final product of 1 km is possible, corresponding to "breakthrough" according to the WMO OSCAR database [RD-1]. Other transient permafrost models are well-established in the community, most notably GIPL 2 (Jafarov et al., 2012) at the University of the Arctic Fairbanks. Transient permafrost models are highly demanding computationally ($>10^6$ more CPU hours compared to an equilibrium model), so that High Performance Computing frameworks must be used. On the other hand, validation with field data is possible in a much stricter way, as ground temperature and thaw depth measured at a specific depth and date can be compared.

3 JUSTIFICATION ON THE ALGORITHM CHOSEN

3.1 User requirements

The Permafrost CCI project gathered existing user requirements from international consensus references, such as GCOS-200, the IGOS Cryosphere theme report (WMO, 2007) and the WMO RRR database (WMO, 2011a), as well as from the climate modelling community through the Modelling Working Group of the Permafrost Carbon network (PCN). The requirements review further covered user survey results from ESA DUE GlobPermafrost, a white paper in the framework of the WMO Polar Space Task Group (Bartsch et al. 2014), workshop reports (e.g. NRC 2014) and discussions with representatives of the International Permafrost Association (IPA) and the IPA Action Group 'Specification of a Permafrost Reference Product in Succession of the IPA Map'. Views from climate researchers associated with the project (AWI, University of Fribourg, West University of Timisoara) were also taken into account, as well as from permafrost researchers in the H2020 project Nunataruyk.

Users demand a combination of extensive geographical coverage (global permafrost region about 20-30 Mio km^2), high spatial resolution (target resolution 1km) including representation of subgrid variability, high temporal resolution (monthly data) and long temporal coverage (one to several decades back in time). These requirements go considerably beyond the state-of-the-art in remote permafrost ECV assessment, based on published studies and recently demonstrated progress. The main requirement for Permafrost CCI is to implement a Permafrost ECV processing system that retains the capabilities (e.g. spatial resolution, assessment of subpixel variability, global coverage) of the GlobPermafrost products, but at the same time can evaluate the transient response of the ground thermal regime to changes in the climatic forcing.

In response to the user requirements and in agreement with GCOS Action T34, the Permafrost_cci project will deliver novel products for ground temperature and active layer thickness, based on the transient permafrost model CryoGrid CCI, which was developed for the project based on the existing CryoGrid 2 model (Westermann et al., 2013; 2017). CryoGrid CCI was originally conceived as a stand-alone model designed to function as part of the Permafrost_cci processing chain. To make it more accessible to a wider user community, CryoGrid CCI has been fully integrated in the CryoGrid community model (Westermann et al., 2023) in CCI4.

3.2 Technical requirements

Apart from specific accuracy and resolution requirements, users have stressed the need for the development of a suitable benchmark dataset, as it does not exist yet to date. While the terrestrial monitoring of permafrost temperatures and active layer thickness has been drastically expanded during and after the "International Polar Year" (IPY), the distribution of sites is strongly biased towards a few regions (typically where resource extraction and/or infrastructure projects have created easy access), leaving vast areas uncovered by monitoring (Biskaborn et al., 2019).

Accuracy requirements stated by the users are strongly complicated by the fact that permafrost ECV physical variables (ground temperature and active layer thickness) feature significant variations at spatial scales much smaller than the target requirement of 1km, which in the few documented cases exceed even the threshold requirement of an RMSE of 2.5K (e.g. Fig. 2 in Gisnås et al., 2014). Therefore, even comparison of "perfect" 1km average temperatures to point temperature measurements in boreholes will feature a significant RMSE which in this case rather reflects the spread of temperatures in space than the accuracy of the method. Furthermore, boreholes are generally not placed at random locations within a pixel, but at sites favourable for drilling, and/or sites where permafrost can be expected, especially in the discontinuous and sporadic permafrost zones. When comparing model results to point-scale measurements, biases introduced by the method/model and the input data will thus be masked by the spatial variability of permafrost parameters, which significantly complicates the evaluation of accuracies.

Since EO-based algorithms necessarily operate at the spatial scale of individual pixels, the spatial resolution of the output must therefore be put in context with the spatial variability of permafrost temperatures and active layer thickness. As ground temperatures vary strongly at spatial scales smaller than the footprint of EO sensors, it is desirable to derive permafrost extent (fraction) as permafrost ECV parameter (in line with the WMO RRR database), which is the aerial fraction within an area (pixel) at which the definition for the existence of permafrost (ground temperature < 0 °C for two consecutive years) is fulfilled. The characterization of the permafrost extent in terms of aerial coverage has been employed for decades in the permafrost community, e.g. in the classic IPA permafrost map displaying classes of continuous, discontinuous, sporadic and isolated permafrost. Furthermore, the ice content in the ground is an important factor for active layer thickness, especially when the active layer deepens in the course of a warming climate. Therefore, a spatially distributed product of ground stratigraphies is required as input to the permafrost model in order to achieve a satisfactory performance for the active layer thickness. Permafrost_cci has created the first transient permafrost extent products for the Northern Hemisphere at spatial resolution of 1km, which are continuously improved as the project evolves.

4 PROCESSING LINE

4.1 The CryoGrid CCI ground thermal model

The CryoGrid family of ground thermal models has been employed for a wide variety of tasks, with the simple equilibrium model CryoGrid 1 (e.g. Westermann et al., 2015) used in ESA GlobPermafrost to compile the first EO-derived global map of permafrost extent and temperatures (Obu et al., 2019; 2020). Other CryoGrid versions are the transient model CryoGrid 2 (Westermann et al. 2013), from which the transient model used in Permafrost_cci, CryoGrid CCI, has been developed. Furthermore, CryoGrid CCI has been supplemented with elements of the more sophisticated land surface scheme CryoGrid 3 (Westermann et al., 2016), as well as the CROCUS snow model (Vionnet et al., 2012). Continued model development with a community of mainly European permafrost researchers recently led to the establishment of a CryoGrid community model (Westermann et al. 2023), which comprises the functionalities of the CryoGrid 1, 2, and 3 models in a modular framework. The CryoGrid community model and the Permafrost_cci CryoGrid CCI model have been developed in parallel for several years, with the community model primarily designed to offer flexibility for a wide range of applications, while CryoGrid CCI was mainly conceived to optimize computation speed within the Permafrost_cci processing line. In CCN4, CryoGrid CCI has been fully integrated as a new module in the CryoGrid community model, making it accessible to a wider user community. This work has added new functionalities to the model toolbox, e.g. modules for generating model ensembles (Sect. 4.1.2) and ingesting spatially distributed data sets (Sect. 4.2), which boosts the capabilities of other types of permafrost simulation tools within the CryoGrid community model. Through this model development, it is now possible to set up the Permafrost_cci processing chain entirely within the CryoGrid community model. In the following, we briefly describe the theoretical bases for CryoGrid CCI. Further details are provided in Westermann et al. (2023), with key equations the same as for the class "GROUND_freeW_ubT" in the Cryogrid community model.

In CryoGrid CCI, the main prognostic state variable, which is integrated in time, is the enthalpy (as in the GIPL2 model; Jafarov et al., 2012), which offers advantages with respect to energy conservation (Westermann et al., 2023). Thus, CryoGrid CCI numerically solved the heat conduction equation in the enthalpy formulation:

$$\frac{dE}{dt} = \frac{d}{dz}\left(K(T(E))\frac{dT(E)}{dz}\right),$$

with E denoting the enthalpy [J/m^3], t time [sec], K the thermal conductivity [W/mK], T temperature [K] and z the vertical space coordinate [m]. The left-hand side of the equation corresponds to the derivative of enthalpy in t time, while the right-hand side corresponds to the divergence (i.e. gradient in one dimension) of the conductive heat flux. The temperature T can be computed from enthalpy using a unique function, which takes into account both the heat capacity and latent heat change effects due freezing/melting of water/ice. The thermal conductivity is again obtained as a function of temperature, as described in Westermann et al. (2023). The heat conduction equation is discretized in space using the method of lines, while we use the simplest possible time integration scheme, first-order forwards Euler (Westermann et al., 2023), to integrate the fields of enthalpy and temperature in time. The main advantage of the enthalpy formulation is that it is by definition satisfies conservation of energy for the given heat fluxes. Furthermore, the enthalpy variable does not feature a strong discontinuity at the freezing point of water, 0°C, as it is the case when temperature is used as state variable in the time integration. The soil freezing characteristic, i.e. the function temperature vs. enthalpy, is parametrized analogous to many Earth system models (e.g. Gouttevin et al., 2012), with a freezing range between 0°C and a predefined freezing temperature T$_{freeze}$, between which the phase change of water/ice is assumed to occur. While this is only a simplification of a real soil freezing characteristic, it features strong advantages in particular with respect to model runtime. Furthermore, the method allows for a consistent treatment of free water/ice, which allows full continuity between the treatment of the ground and the snow cover.
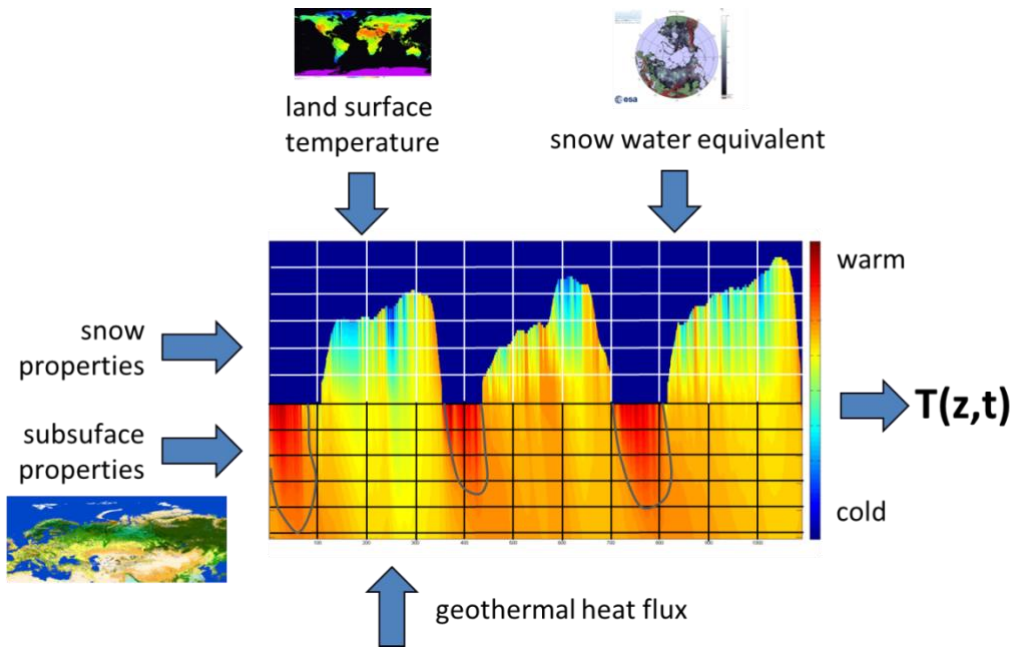
Figure 1: *Schematic representation of the CryoGrid CCI model scheme, showing the input data land surface temperature and snow water equivalent flow which time series are required. Snow properties are computed by the model scheme, while subsurface properties are assigned based on the ESA CCI landcover product. At the lower boundary of the model domain, a (constant) geothermal heat flux is prescribed. CryoGrid CCI delivers depth- and time-resolved fields of ground temperatures, from which annual averages at different depths, as well as annual active layer thickness (from thaw progression, grey line).*

4.1.1 Snow model

A major challenge for spatially distributed application of thermal models is the snow cover, which insulates the ground from the colder atmospheric temperatures in winter. Especially the snow density is a challenging parameter, as it is highly variable in space, but determines both snow depth (if snow water equivalent is provided) and the thermal conductivity of the snow cover. In regional studies, the snow density is mostly prescribed based on field measurements (e.g. Westermann et al., 2013; 2017), but this method already fails for larger regions with stronger environmental gradients (e.g. Nicolsky et al., 2017), making global application essentially impossible without factoring in the main drivers for snow depth. In CryoGrid CCI, we employ a snow compaction model oriented at the CROCUS scheme, taking into account a temperature- and wind-speed dependent initial snow density, snow compaction due to the overburden of overlying snow layers, as well as compaction by wind drift (see Vionnet et al., 2012). The scheme is a simplified version of the snow module based on CROCUS implemented in the CryoGrid community model (Westermann et al., 2023). Note that a fully-fledged snow model like CROCUS can not be applied within the Permafrost_cci processing line, as this would require explicitly solving the surface energy balance, instead of relying on remotely sensed data sets. Three snow layers are employed

in CryoGrid CCI, of which the first layer is impacted by wind compaction. Phenomenologically, the goal of the snow scheme is to reproduce observed large-scale gradients of the snow density, i.e. snow density increases with snow water equivalent, temperature and windiness, which have already been accounted for in the ESA GlobPermafrost project (in this case using the formulation of Onuchin and Burenina, 1996). However, an advantage of the CryoGrid CCI snow scheme is that snow densities can change over time in response to the applied model forcing.

4.1.2   Ensemble generation

For each 1km pixel, time series of surface temperature, snowfall and snowmelt are provided. To estimate the spatial variability of ground temperature and active layer thickness within a pixel, we generate an ensemble corresponding to the best guess for equal-area subpixel fractions, taking a range of factors into account. For ensemble generation, we first use subpixel landcover fractions to define a stratigraphies for each ensemble member, according to the fractional coverage of landcover classes (see below). Note that landcover classes with low fractions are not accounted for if the number of ensemble members is not sufficient. For each landcover class present, snowfall is further scaled according to a lognormal distribution function, using coefficients of variations that are again dependent on landcover (according to Liston, 2004). This way, the natural variability of snow depths which gives rise to strong small-scale differences of ground temperatures especially in tundra areas (e.g. Gisnås et al., 2014) is accounted for in a statistical way. Note that it is at this point not possible to take subpixel variability of land surface temperature (LST) into account, as EO-derived LST products can only provide a single average value for 1km pixels. This is a limitation especially in mountain areas in mid-latitudes where the small-scale variability of slopes and aspects is a key factor for permafrost distribution.

4.1.3   Model operation and technical aspects

The vertical model domain extends to a depth of 100m below the surface, with a vertical discretization of 0.1 m within the uppermost 1.5 m to resolve the active layer in detail. In deeper layers, discretization gradually increases up to a spacing of 10 m for the lowermost grid cells. A constant model time step of 1 hour (3600 sec) is employed in the time routine, which simplifies massively parallel application as required in Permafrost_cci. Model initialization follows the computationally accelerated step-wise spin-up procedure outlined in Westermann et al. (2023), which can estimate both the steady-state thermal gradient in deeper layers and the "transient" steady-state in the upper layers. For this purpose, we use ERA-5 reanalysis data for the five-year period 1980 to 1984, but with average values adapted to ERA-5 data from the 30-year period 1950 to 1979, so that the model spin-up reflects the average climate

conditions for this earliest period for which reliable reanalysis data are available. With the model initialized to this 1950 to 1979 state, transient runs are performed with data from 1980 until 1997, allowing for an additional spin-up period of 17 years. It must be emphasized air temperatures from ERA-5, which drive the model at its upper boundary, are downscaled with MODIS LST data for the overlap period 2003 to 2021 (Sect. 4.2.1), so that the information from these EO data sets is contained in the entire model run, including the model spin-up.

4.2   Pre-processing

Due to availability of the remote sensing data sets, the processing line is set for the period 2003 to 2023 in CCI4 iteration 2. The spatial resolution is 1km, in line with user requirements. The processing chain starts with pre-processing of forcing data sets for the CryoGrid CCI thermal model, which are compiled as eight-day averages to drive the model. In the second step, the CryoGrid CCI thermal model is run in ensemble mode (i.e. simulating a number of different realizations for each pixel), using predefined distributions for the snow and higher (300m) resolution data for landcover as input. Finally, postprocessing of the model output leads to generation of the Permafrost_cci data sets for the Permafrost ECV physical variables ground temperature and active layer thickness. In addition, ensemble mode (as demonstrated in ESA Globpermafrost) can deliver permafrost probabilities/ fractions demanded by the user community.

4.2.1 Land surface temperature

Until CCN4 iteration 1, Land surface temperatures (LST) from the daily level 3 version 6 MODIS LST collections MOD1A11/MYD1A11 (both Terra and Aqua satellites) were employed as input for the Permafrost_cci processing chain. If available for the target period 2003-2023, these will be replaced by the corresponding ESA LST_cci and C3S data sets in CCI4 iteration 2 which are provided at 0.01 degree resolution in geographic coordinates. For cloud-free skies, these feature up to four values per day (one day and night-time value for each satellite). The overpass time is variable, as the overpass closets to nadir is selected for which the scene is free of clouds.

In high-latitude regions, prolonged periods of cloudiness constitute a major challenge for remotely sensed LST, and validation studies have demonstrated a considerable bias of several Kelvin for longer-term (weekly to seasonal) LST averages inferred from satellites (Langer et al., 2010; Westermann et al. 2011; 2012; Østby et al., 2014). For this reason, it is crucial to gap-fill the LST time series during cloudy periods. In Permafrost_cci, we follow the successful gap-filling approach taken in Westermann et al., 2015 and ESA Globpermafrost, which uses air temperatures from the ERA reanalysis for gap-filling.

Other than in ESA GlobPermafrost, Permafrost_cci benefits from the much improved ERA-5 reanalysis which covers the entire time period and offers improved spatial and vertical resolution of the atmospheric model. The coarse-scale (~30km) reanalysis data are first downscaled to 1km resolution using a Digital Elevation Model, relying on information from different pressure levels to account for atmospheric lapse rates in the target regions (see Westermann et al., 2015 for details). Finally, downscaled air temperatures are inserted to fill the gaps in the MODIS LST time series, using the actual timestamp of the MODIS retrieval to define the gaps. From the combined time series, eight-day (8d) LST averages are computed, which are used to force the CryoGrid CCI thermal model.

4.2.2 Snow cover

To take the insulating effect of the seasonal snow cover on the ground thermal regime into account, time series of snow depths are required in thermal modelling. Time series derived from space-borne passive microwave sensors have been employed to drive thermal models for a small region in Siberia (Westermann et al., 2017), but work in the ESA GlobPermafrost showed major deficits especially in mountain and coastal areas, as well as in areas with a high fraction of water bodies. These findings are in line with major validation studies (e.g. Takala et al., 2013; see also open discussion of Westermann et al., 2017). Furthermore, the coarse spatial resolution of ~25km would strongly decrease the final resolution of Permafrost_cci products below threshold resolution [RD-1], and compromise acceptance in the permafrost community. Similar to ESA GlobPermafrost, we use a physically-based snow model driven by downscaled reanalysis data in year 1 to overcome these problems, leading to a snow data at a spatial resolution matching the LST input data sets (1km). Snowfall data sets are generated by downscaling ERA-5 precipitation fields with altitude (5% increase per 1000m) and applying a threshold criterion of 0°C of the downscaled air temperatures (see above). For the melt rate, a degree-day based melt model has been applied in in years 1-3 of Permaforst_cci, but this has been supplemented by a simple surface energy balance formulation since CCI4 iteration 1. While sensible heat fluxes are again derived from a degree-day approach using downscaled air temperatures from ERA-5, incoming short- and longwave radiation are explicitly accounted for. These are again derived from ERA-5 and downscaled for the altitude of each 1km model grid cell using the TopoScale approach (Fiddes and Gruber, 2014). The snow albedo is parameterized as in the simple snow model in the CryoGrid community model (which is the same approach as used in CryoGrid 3, Westermann et al., 2016), with the albedo decaying from a maximum value for fresh snow (set to 0.85) to a minimum value for old snow (set to 0.5) with independent decay coefficients for dry and wet (i.e. melting) snow. Both snowfall and melt are accumulated for the same eight day periods as the LST forcing.

In CCN4 iteration 2, we will test a data assimilation procedure using remotely sensed "fractional snow covered area" to correct the ERA5-derived snowfall on a pixel-by-pixel basis (as in Aalstad et al., 2018) for tundra areas without forest cover. Depending on the performance and consistency considerations with respect to the forested areas (e.g. artefacts along boundaries between forested and non-forested areas), we will include the data assimilation procedure in the processing chain or not.

4.2.3 Land cover and subsurface information

To apply spatially distributed data sets of surface and subsurface parameters, a spatial classification is required. As in ESA GlobPermafrost, Permafrost_cci will rely on the Landcover_cci classification at 300m resolution, aggregating classes to seven "super-classes": bare, vegetated tundra, grassland, shrub, coniferous forest, deciduous forest and wetland, as well as Yedoma tundra and Yedoma forest. The Yedoma extent is based on binary Yedoma maps produced by AWI, which are subsequently intersected with the Landcover_cci derived landcover classes. For application in ensemble mode of CryoGrid CCI, we calculate the areal fractions of each super-class for each 1km pixel.

For application of any thermal subsurface model, a stratigraphy of subsurface thermal parameters must be defined for the entire vertical model domain (see above). In CryoGrid CCI, we use the parametrizations originally developed in CryoGrid 2 (Langer et al., 2013; Westermann et al., 2013; 2017) and implemented in the CryoGrid community model which allows translating volumetric fractions of the mineral, organic, air and water/ice phases within the ground to the "native " model parameters heat capacity and thermal conductivity (see above). The advantage of this method is that the abundance of field data sets on these parameters can be employed in modelling, using data from soil cores and pits, as well as exposed sections along river banks and construction sites. To define stratigraphies for each model grid cell, we use a novel stratigraphy product based on Landcover_cci and in-situ observations of ground stratigraphies for different landcover classes. For this purpose, stratigraphies were generated from approx. 6500 samples from 700 pedons. The pedons were distributed across the Arctic in Siberia (Spasskaya Pad, Lena Delta, Kytalyk, Shalaurovo, Cherskii, Taymyr and Seida), Northern America (Tulemalu Lake, Richardsson Mountains, Ogilvi Mountains, Herschel Island), Scandianvia (Abisko and Tarfala valley), Greenland (Zackenberg) and Svalbard (Adventdalen and Ny-Ålesund). The pedons included organic-rich soils, shallow soils on bedrock, and ice rich ground (Yedoma).

The samples were taken with known volumes, weighed before and after drying and analysed for organic carbon using elemental analyser. Mass of different soil components was calculated first. The mass of water was calculated as a difference between wet and dry sample mass. The organic matter mass was obtained by multiplying dry sample weight and mass of organic matter multiplied by two, which is a

conversion factor between SOC and SOM (Pribyl, 2010). The mass of the mineral material was calculated as the dry sample mass minus the organic matter mass. Fractions of volumetric contents for each of the components were calculated by dividing volume of component with a total volume of sample. The component volumes were calculated from mass by assuming the following densities: 1 g/cm^3 for water; 1.3 g/cm^3 for organic matter (Farouki, 1981); 2.65 g/cm^3 for mineral material in soil (Hillel, 2003). The volumetric fraction of the air phase was calculated as the remaining of other fractions from one.
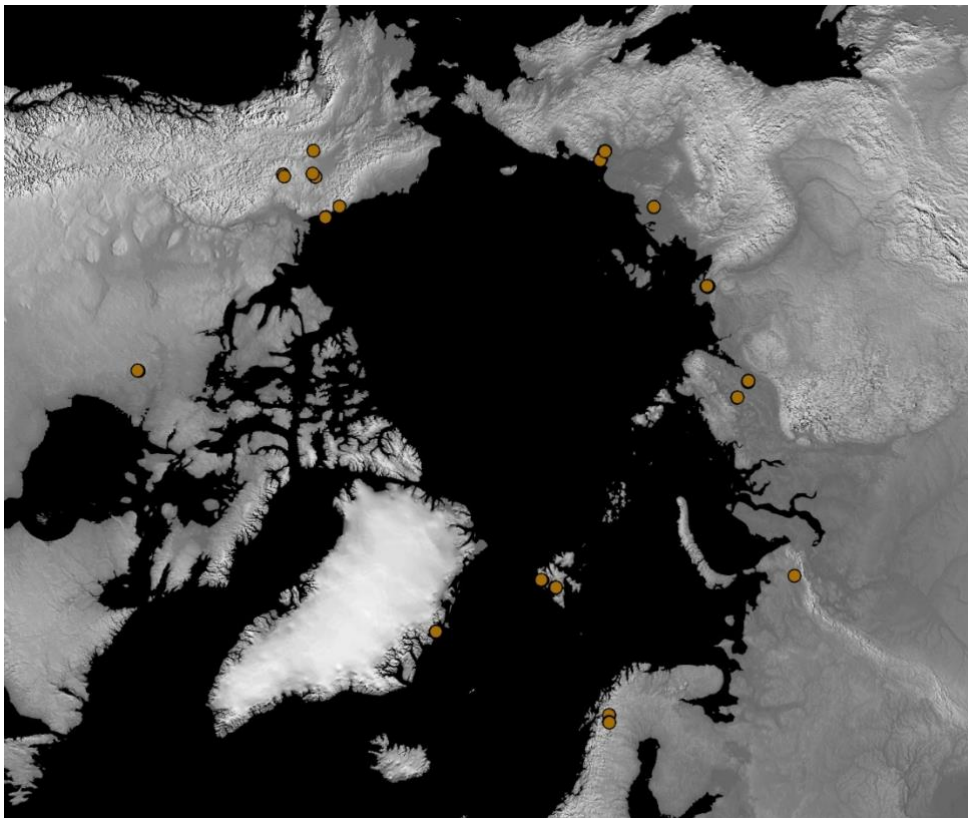

Figure 2: *Distribution of sampling sites for in-situ observations of ground stratigraphies, which were used to generate a spatially distributed product of ground stratigraphies as input to the CryoGrid CCI permafrost model.*

The pedons were grouped according to land cover classes recognised in the field. Average was calculated for each centimetre of soil column and standard deviation was used to create ranges of possible values for each landcover. Generated Soil columns were grouped again to seven depths using hierarchically constrained clustering to be suitable as model input. Fig. 3 shows the resulting depth distribution for the mineral fraction for different landcover classes.
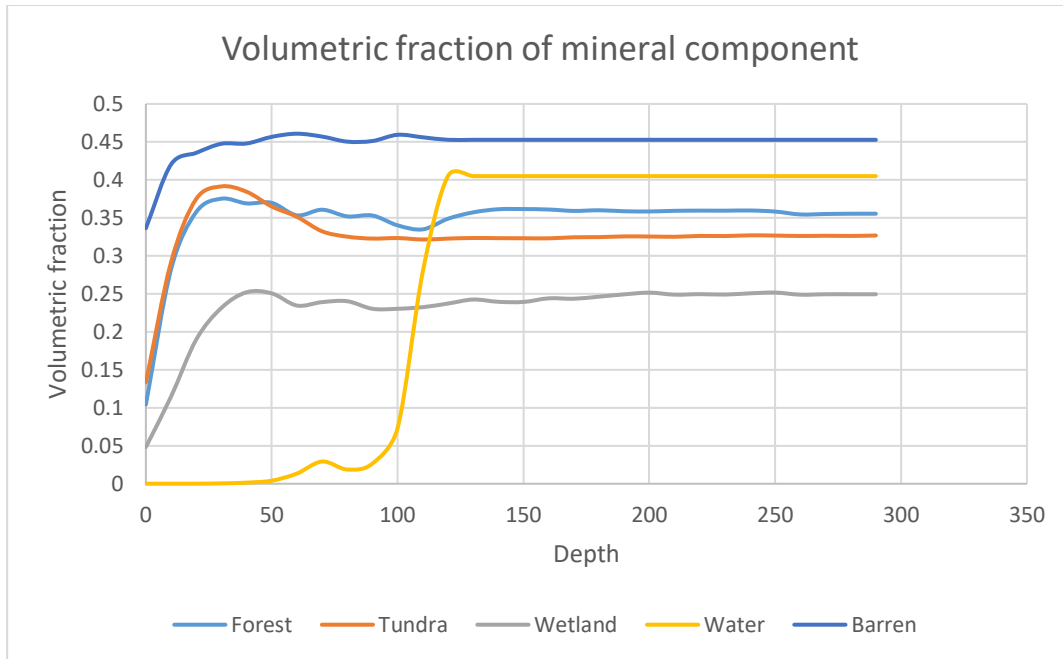
Figure 3: *Depth distribution of the volumetric fraction of the mineral constituents of the stratigraphy, as obtained from averaging of available pedons. See text.*

4.3 Post-processing

For each ensemble member, the resulting ground temperature field (in time and depth) is averaged over yearly periods for different depths (1m, 2m, 5m, 10m and 20 m), and the active layer thickness is determined as the depth of maximum thaw within each year. For each pixel, we the determine both mean and the standard deviation of temperatures. The standard deviation provides a robust first-order assessment of the uncertainty of the mean, corresponding to the expected spread in ground temperatures when measuring at a random location within a pixel. As Permafrost_cci is strongly directed towards the climate modelling community, which in general uses only a single realization for a grid cell, the ensemble spread is exploited for the characterization of uncertainties for both ground temperatures and active layer thickness. Furthermore, the ensemble allows to calculate the fractional permafrost cover which makes it possible to produce maps with the well-known permafrost zonation in continuous, discontinuous and sporadic permafrost. To infer the permafrost fraction within each pixel, we explicitly check for each ensemble member if the first cell below the seasonal thaw layer (characterized by having both positive and negative ground temperatures) is constantly below the freezing point. While formally correct, this method classifies short-term freezing of an upper ground layer due to an extended period of cold years as permafrost (in accordance with the formal definition), although an unfrozen zone exists

below the shallow frozen layer. With permafrost presence inferred for each ensemble member, permafrost fractions can be calculated. Note that despite the low number of ensemble members (7), an estimate for the permafrost zonations can be obtained, with continuous permafrost corresponding to all 7 realizations featuring permafrost, discontinuous to 4-6, sporadic to 1-3, while a pixel is flagged as permafrost-free if none of the ensemble members features permafrost.

5   REQUIRED INPUT DATA

Permafrost_cci level 4 products are created from the analysis of lower level data, resulting in gridded, gap-free products [RD-2]. Permafrost_cci will employ remotely sensed Land Surface Temperature, snow cover and landcover data sets, in conjunction with downscaled ERA-5 reanalysis data [RD-3]. Auxiliary data include ground stratigraphies from field investigations, as well as model parameterizations for crucial permafrost and snow processes.

Daily 1km MODIS LST data sets from 2003-2023 based on the level 3 version 006 collection (products MOD11A1 and MYD11A1) have been employed. These data are based on acquisitions of two satellites, Terra and Aqua, which in total provide four measurements per day for cloud-free conditions (two day and night retrievals each). If available for the full period 2003-2023, these will be replaced by the corresponding data sets from ESA LST_cci/C3S in CCN4 iteration 2. Gap-filling as demonstrated in Westermann et al. (2015; 2017) and in ESA GlobPermafrost is accomplished using ERA-5 reanalysis data which are downscaled to 1km resolution with the help of a digital elevation model (see below). Land cover information is required to define soil properties and snow redistribution (Westermann et al. 2015), and the ESA Landcover_cci product will be employed For downscaling of the ERA reanalysis data, a global digital elevation model is required which includes the Arctic and provides sufficient spatial resolution. The 1 km Global Multi-resolution Terrain Elevation Data 2010 (GMTDEM) complies to these requirements. From the ERA-5 reanalysis, surface fields for air temperature, precipitation, geopotential and wind speed are required, as well as air temperature, wind speed and geopotential at the pressure levels 800, 500 and 200mbar.

6 OUTPUT PRODUCTS

The primary variables requiring climate-standard continuity as defined by GCOS are ground temperature and active layer thickness. In addition, permafrost fraction and zone are secondary parameters, but of high interest to users. At product level 4, annual averages of ground temperature and annual maxima of thaw depth (active layer thickness) will be provided at 1km spatial resolution during Permafrost_cci. The output products address the main user requirements [RD-1], including those expressed by the Permafrost_cci climate research group (CRG). All datasets will be provided in NetCDF format.

7   ERROR BUDGET ESTIMATES AND EXPECTED ACCURACY

Here, we specify how product uncertainties are estimated reflecting the combination of sources of uncertainty. These include both the pre-processing of input data sets, the uncertainty propagation through the ground thermal model CryoGrid CCI, as well as additional model uncertainty due to neglected processes. In CryoGrid CCI, uncertainty characterization mainly relies on the spread of permafrost parameters within the model ensemble, which provides a pixel-by-pixel uncertainty accounting for two key sources of uncertainty, i.e. the landcover products and the spatial variability of the snow cover. This procedure in particular captures the dependence of these uncertainties on the climatic properties of a site, e.g. the snow-related uncertainty of ground temperatures is much higher in areas with continental climate/cold winters compared to areas with maritime climate/warm winters.

In principle, the uncertainty could be evaluated more thoroughly through ensemble methods, i.e. by drawing a randomized ensemble of model realizations perturbing input data sets and model parameters according to provided uncertainty characteristic of these data sets. This has been demonstrated in the study by Langer et al. (2013) for a site in Northern Siberia. However, the problem is that permafrost areas are mainly situated in high latitudes and in high mountain areas, for which characterizations of uncertainties of input data sets are often not applicable. This has been demonstrated for MODIS land surface temperature for which much higher uncertainties have been found in Arctic settings compared for benchmark sites typically located in mid-latitudes (Westermann et al. 2011; 2012; Østby et al., 2013). Therefore, automatic uncertainty characterization based on provided uncertainties of input data sets cannot provide meaningful characterization of uncertainties for the Permafrost ECV products. In a few cases, it could be possible to establish additional uncertainty benchmarks of input data sets (e.g. land surface temperature or landcover) for permafrost sites, but a comprehensive evaluation is not possible due to the scarcity of validation sites for many parameters.

8 PRACTICAL CONSIDERATIONS FOR IMPLEMENTATION

Computational costs are one of the principal challenges of the transient Permafrost_cci algorithm, with CryoGrid CCI application for the entire global permafrost domain in ensemble mode being considerably larger than previous applications of transient permafrost models (e.g. Jafarov et al., 2012; Westermann et al., 2013). For this reason, a scalable implementation of the algorithm on the Saga Supercomputing cluster located in Trondheim, Norway, has been chosen, and the model code has been strongly improved with respect to runtime. The entire permafrost domain (ca. 25 Mio km^2) can be simulated for the period 1997-2023 with five ensemble members per grid cell for a computational cost of about 250,000 CPU hours, which makes it possible to produce the Permafrost_cci products at the specifications outlined in [RD-6].

A major challenge is that the considerable processing time (1-2 months depending on load of the HPC cluster), which leads to long turnover cycles and considerably complicates model tuning to achieve an optimal performance. Ongoing improvements of model input data sets are not ingested continuously, but the improvements only become apparent in the next model iteration.

9 REFERENCES

9.1 Bibliography

Aalstad, K., Westermann, S., Schuler, T. V., Boike, J., & Bertino, L., 2018. Ensemble-based assimilation of fractional snow-covered area satellite retrievals to estimate the snow distribution at Arctic sites. *The Cryosphere*, 12(1), 247-270.

Bartsch, A., Höfler, A., Kroisleitner, C., Trofaier, A.M., 2016a. Land Cover Mapping in Northern High Latitude Permafrost Regions with Satellite Data: Achievements and Remaining Challenges. *Remote Sens.*, 8, pp.979.

Bartsch, A., Widhalm, B., Kuhry, P., Hugelius, G., Palmtag, J., and Siewert, M. B. (2016b): Can C-band synthetic aperture radar be used to estimate soil organic carbon storage in tundra?, *Biogeosciences*, 13, 5453-5470, https://doi.org/10.5194/bg-13-5453-2016, 2016.

Biskaborn, B. K., Smith, S. L., Noetzli, J., Matthes, H., Vieira, G., Streletskiy, D. A., Schoeneich, P., Romanovsky, V. E., Lewkowicz, A. G., Abramov, A., Allard, M., Boike, J., Cable, W. L., Christiansen, H. H., Delaloye, R., Diekmann, B., Drozdov, D., Etzelmüller, B., Grosse, G., Guglielmin, M., Ingeman-Nielsen, T., Isaksen, K., Ishikawa, M., Johansson, M., Johannsson, H., Joo, A., Kaverin, D., Kholodov, A., Konstantinov, P., Kröger, T., Lambiel, C., Lanckman, J.-P., Luo, D., Malkova, G., Meiklejohn, I., Moskalenko, N., Oliva, M., Phillips, M., Ramos, M., Sannel, A. B. K., Sergeev, D., Seybold, C., Skryabin, P., Vasiliev, A., Wu, Q., Yoshikawa, K., Zhelezniak, M., and Lantuit, H., 2019. Permafrost is warming at a global scale, *Nature communications, 10,* pp. 1–11.

Farouki, O. T., 1981. Thermal Properties of Soils, COLD REGIONS RESEARCH AND ENGINEERING LAB HANOVER NH. [online] Available from: https://apps.dtic.mil/docs/citations/ADA111734 (Accessed 19 November 2019).

Fiddes, J. and Gruber, S., 2014. TopoSCALE v.1.0: downscaling gridded climate data in complex terrain. *Geoscientific Model Development, 7*, pp. 387–405.

Gisnås, K., Westermann, S., Schuler, T.V., Litherland, T., Isaksen, K., Boike, J. and Etzelmüller, B., 2014. A statistical approach to represent small-scale variability of permafrost temperatures due to snow cover. *The Cryosphere*, *8*, pp.2063-2074.

Gouttevin, I., Krinner, G., Ciais, P., Polcher, J. and Legout, C., 2012. Multi-scale validation of a new soil freezing scheme for a land-surface model with physically-based hydrology. *The Cryosphere*, *6*, pp.407-430.

Hillel, D.: Introduction to environmental soil physics, Elsevier., 2003.

Hugelius, G., Tarnocai, C., Broll, G., Canadell, J.G., Kuhry, P. and Swanson, D.K., 2013. The Northern Circumpolar Soil Carbon Database: spatially distributed datasets of soil coverage and soil carbon storage in the northern permafrost regions. *Earth System Science Data*, *5*(1), pp.3-13.

Jafarov, E.E., Marchenko, S.S. and Romanovsky, V.E., 2012. Numerical modeling of permafrost dynamics in Alaska using a high spatial resolution dataset. *The Cryosphere*, *6*(3), pp.613-624.

Langer, M., Westermann, S. and Boike, J., 2010. Spatial and temporal variations of summer surface temperatures of wet polygonal tundra in Siberia-implications for MODIS LST based permafrost monitoring. *Remote Sensing of Environment*, *114*(9), pp.2059-2069.

Langer, M., Westermann, S., Heikenfeld, M., Dorn, W. and Boike, J., 2013. Satellite-based modeling of permafrost temperatures in a tundra lowland landscape. *Remote Sensing of Environment*, *135*, pp.12-24.

Liston, G.E., 2004. Representing subgrid snow cover heterogeneities in regional and global models. *Journal of climate*, *17*(6), pp.1381-1397.

Nicolsky, D.J., Romanovsky, V.E., Panda, S.K., Marchenko, S.S. and Muskett, R.R., 2017. Applicability of the ecosystem type approach to model permafrost dynamics across the Alaska North Slope. *Journal of Geophysical Research: Earth Surface*, *122*(1), pp.50-75.

Obu, J., Westermann, S., Bartsch, A., Berdnikov, N., Christiansen, H. H., Dashtseren, A., Delaloye, R., Elberling, B., Etzelmüller, B., Kholodov, A., Khomutov, A., Kääb, A., Leibman, M. O., Lewkowicz, A. G., Panda, S. K., Romanovsky, V., Way, R. G., Westergaard-Nielsen, A., Wu, T., Yamkhin, J., and Zou, D., 2019. Northern Hemisphere permafrost map based on TTOP modelling for 2000–2016 at 1 km2 scale. *Earth-Science. Review, 193*, pp. 299–316.

Obu, J., Westermann, S., Vieira, G., Abramov, A., Balks, M. R., Bartsch, A., Hrbácek, F., Kääb, A., and Ramos, M. 2020. Pan-Antarctic map of near-surface permafrost temperatures at 1 km2 scale. *The Cryosphere, 14*, pp497–519.

Onuchin, A.A. and Burenina, T.A., 1996. Climatic and geographic patterns in snow density dynamics, Northern Eurasia. *Arctic and Alpine Research*, *28*(1), pp.99-103.

Pribyl, D. W.: A critical review of the conventional SOC to SOM conversion factor, Geoderma, 156(3), 75–83, doi:10.1016/j.geoderma.2010.02.003, 2010.

Reschke, J.; Bartsch, A.; Schlaffer, S.; Schepaschenko, D. Capability of C-Band SAR for Operational Wetland Monitoring at High Latitudes. *Remote Sens*. 2012, 4, 2923-2943.

Vionnet, V., Brun, E., Morin, S., Boone, A., Faroux, S., Le Moigne, P., Martin, E. and Willemet, J.M., 2012. The detailed snowpack scheme Crocus and its implementation in SURFEX v7. 2. *Geoscientific Model Development*, *5*, pp.773-791.

Westermann, S., Langer, M. and Boike, J., 2011. Spatial and temporal variations of summer surface temperatures of high-arctic tundra on Svalbard—implications for MODIS LST based permafrost monitoring. *Remote Sensing of Environment*, *115*(3), pp.908-922.

Westermann, S., Langer, M. and Boike, J., 2012. Systematic bias of average winter-time land surface temperatures inferred from MODIS at a site on Svalbard, Norway. *Remote Sensing of Environment*, *118*, pp.162-167.

Westermann, S., Schuler, T., Gisnås, K. and Etzelmuller, B., 2013. Transient thermal modeling of permafrost conditions in Southern Norway. *The Cryosphere*, *7*(2), pp.719-739.

Westermann, S., Østby, T.I., Gisnås, K., Schuler, T.V. and Etzelmüller, B., 2015. A ground temperature map of the North Atlantic permafrost region based on remote sensing and reanalysis data. *The Cryosphere*, *9*(3), pp.1303-1319.

Westermann, S., Langer, M., Boike, J., Heikenfeld, M., Peter, M., Etzelmüller, B. and Krinner, G., 2016. Simulating the thermal regime and thaw processes of ice-rich permafrost ground with the land-surface model CryoGrid 3. *Geoscientific Model Development*, *9*(2), pp.523-546.

Westermann, S., Peter, M., Langer, M., Schwamborn, G., Schirrmeister, L., Etzelmüller, B. and Boike, J., 2017. Transient modeling of the ground thermal conditions using satellite data in the Lena River delta, Siberia. *The Cryosphere*, *11*(3), pp.1441-1463.

Westermann, S., Ingeman-Nielsen, T., Scheer, J., Aalstad, K., Aga, J., Chaudhary, N., Etzelmüller, B., Filhol, S., Kääb, A., Renette, C., Schmidt, L. S., Schuler, T. V., Zweigel, R. B., Martin, L., Morard, S., Ben-Asher, M., Angelopoulos, M., Boike, J., Groenke, B., Miesner, F., Nitzbon, J., Overduin, P., Stuenzi, S. M., and Langer, M., 2012. The CryoGrid community model (version 1.0) – a multi-physics toolbox for climate-driven simulations in the terrestrial cryosphere. *Geoscientific Model Development, 16*. pp. 2607–2647.

Østby, T.I., Schuler, T.V. and Westermann, S., 2014. Severe cloud contamination of MODIS land surface temperatures over an Arctic ice cap, Svalbard. *Remote Sensing of Environment*, *142*, pp.95-102.

8.2 Acronyms

AD	Applicable Document
ALT	Active Layer Thickness
AWI	Alfred Wegener Institute Helmholtz Centre for Polar and Marine Research
B.GEOS	b.geos GmbH

CCI	Climate Change Initiative
CDR	Climate Data Record
CRG	Climate Research Group
CRS	Coordinate Reference System
DARD	Data Access Requirements Document
ECV	Essential Climate Variable
EO	Earth Observation
ESA	European Space Agency
ESA DUE	ESA Data User Element
GAMMA	Gamma Remote Sensing AG
GCOS	Global Climate Observing System
GCMD	Global Change Master Directory
GIPL	Geophysical Institute Permafrost Laboratory
GTD	Ground Temperature at certain depth
GTN-P	Global Terrestrial Network for Permafrost
GUIO	Department of Geosciences University of Oslo
IPA	International Permafrost Association
IPCC	Intergovernmental Panel on Climate Change
LST	Land Surface Temperature
MAGT	Mean Annual Ground Temperature
MAGST	Mean Annual Ground Surface Temperature
NetCDF	Network Common Data Format
NSIDC	National Snow and Ice Data Center
PFR	Permafrost extent (Fraction)
PFF	Permafrost-Free Fraction
PFT	Permafrost underlain by Talik
PSD	Product Specifications Document
PSTG	Polar Space Task Group
PZO	Permafrost Zone
RD	Reference Document
RMSE	Root Mean Square Error
RS	Remote Sensing
SLF	Institut für Schnee- und Lawinenforschung, Davos
SU	Department of Physical Geography Stockholm University
TSP	Thermal State of Permafrost
UAF	University of Alaska, Fairbanks
UNIFR	Department of Geosciences University of Fribourg
URD	User Requirements Document
WGS 84	World Geodetic System 1984
WUT	West University of Timisoara